NRIAG Journal of Astronomy and Geophysics (2016) 5, 313–322

National Research Institute of Astronomy and Geophysics

NRIAG Journal of Astronomy and Geophysics

www.elsevier.com/locate/nrjag

Visualizing geoelectric – Hydrogeological parameters of Fadak farm at Najaf Ashraf by using 2D spatial interpolation methods

Wadhah Mahmood Shakir Al-Khafaji [a,*], Hayder Abdul Zahra Al-Dabbagh [b]

[a] *University of Baghdad, College of Science for Women, Dept. of Physics, Iraq*
[b] *Ministry of Science and Technology, Dept. of Geophysics, Iraq*

Received 18 February 2016; revised 24 April 2016; accepted 11 July 2016
Available online 23 September 2016

KEYWORDS

Spatial interpolation;
Fadak farm;
Groundwater;
Resistivity method;
Schlumberger;
Aquifer characteristics

Abstract A geophysical survey achieved to produce an electrical resistivity grid data of 23 Schlumberger Vertical Electrical Sounding (VES) points distributed across the area of Fadak farm at Najaf Ashraf province in Iraq. The current research deals with the application of six interpolation methods used to delineate subsurface groundwater aquifer properties. One example of such features is the delineation of high and low groundwater hydraulic conductivity (K). Such methods could be useful in predicting high (K) zones and predicting groundwater flowing directions within the studied aquifer. Interpolation methods were helpful in predicting some aquifer hydrogeological and structural characteristics. The results produced some important conclusions for any future groundwater investment.

1. Introduction

Aquifer resistivity 2D spatial interpolation filtering methods were used in order to reduce noise related to mapping resistivity data. Therefore, it was proposed to draw maps by using some of these techniques with better visualization and differentiation between the low and high groundwater flowing zones of the studied aquifers within the study area.

There were 4 boreholes drilled at the southern part of the study area. The wells at the middle part of the area are artesian and some natural springs show up in the area. Pumping tests were achieved near the (VES) points 19, 21, 22 and 23. The pumping test results were statistically helpful in correlating between the geoelectrical and hydrogeological parameters. The obtained hydrogeological parameters by the pumping tests are the hydraulic conductivity (K) and Transmissivity (T_r). Empirical relations were conducted between aquifer resistivity ($\rho_{Aq.}$) and (K), and, between ($\rho_{Aq.}$) and (T_r), are used to get more information about the aquifer characteristics that could help to select the best location of water well of economic importance in the future.

* Corresponding author.

Peer review under responsibility of National Research Institute of Astronomy and Geophysics.

Production and hosting by Elsevier

http://dx.doi.org/10.1016/j.nrjag.2016.07.001
2090-9977 © 2016 Production and hosting by Elsevier B.V. on behalf of National Research Institute of Astronomy and Geophysics.

Furthermore, when dealing with the aquifer as an isolated electrical zone, it was possible to apply the polynomial regression method which was proposed to isolate low and high residual resistivities within the aquifer. This gave indications about the satisfactory locations of high (K) values within the area for any future groundwater domestic investment.

2. Location and geology of the area

The resistivity surveyed area represents Fadak farm which was located at Najaf Ashraf province, SW Iraq. The area is bounded by the coordinates: (Latitudes: 31°58′00″–32°02′00″ N; Longitudes: 44°00′00″–44°05′00″E). Fig. 1 shows the location and geology of the study area.

The study area is located 35 km from the center of Najaf province. The area is bounded by Rahima-AlRuhban road from the north, and Ain Al Jamal from the south. Also, it is bounded by Al Mustraha springs and sand dunes from the east, and Faidhat AlQar, Ain AlNassar from the west. The area is considered as a part of Al Salman zone within the stable shelf, close to the transition zone from stable to unstable zone. Dammam Formation exposed at the surface is of Upper and Middle Eocene and represented by neritic depositional environment; and mainly consists of carbonate rocks (limestone and Dolomite), with Nummulites (Barawary and Slewa,1994). In subsurface this formation extends to cover wide area of the western and southern desert of Iraq and considered by many as the important groundwater aquifer. According to (Jassim and Goff, 2006), Dammam formation is in unconformable lies beneath Furat Formation rocks, Russ Formation. Dammam Formation has a thickness of (150–200 m) in the study area.

Structurally, the area is located within a zone affected by three types of faults. The NS deep faults of Early Cambrian, the NE-SW normal faults of Late Cambrian to Mesozoic represent the most prevailing faulting direction in the study area where most of seasonal valleys flow in this direction. And finally, the long NW-SE long extending faults of Mesozoic to Tertiary activity period when Najd mountains formed (Buday and Jassim, 1987).

3. Overview of resistivity methods

The most commonly used methods for measuring earth resistivity are those in which current is driven through the ground by using four electrodes. AC current is driven through one pair of electrodes and the potential is measured by second pair of electrodes (Keller and Frischknecht, 1966).

Such surface resistivity methods have been efficiently used for groundwater exploration for many years. Earth resistivities are related to important geologic parameters of the subsurface including types of rocks and soils, porosity, and degree of saturation (Keller and Frischknecht, 1966; Batayneh, 2009).

From the magnitude of the current applied and from the knowledge of the current electrode separation it is possible to calculate the potential distribution and the path of the current flow if the underground was homogeneous. Anomalous conditions or inhomogeneities within the ground, such as electrically better or poorer conducting layers, are inferred from the fact that they deflect the current and distort the normal potentials (Sharma, 1986).

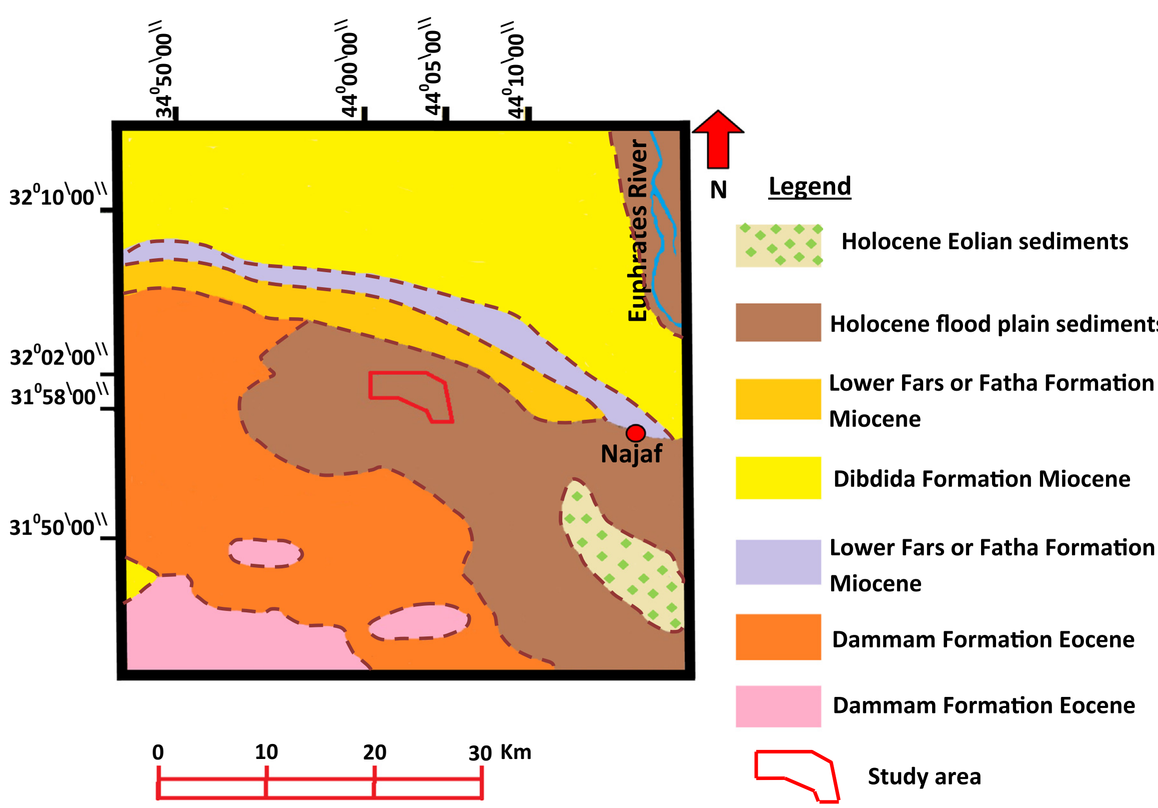

Figure 1 The location and geology of the study area.

With the exception of clays and certain metallic ores, the passage of electricity through rocks takes place by way of the groundwater filling partially or totally the pores and fissures, while the rock matrix being nonconducting, i.e. resistivity increases with decrease in the amount of water in the pore spaces and fissures. All other factors being constant an increase in the concentration of dissolved salts in the groundwater leads to decrease in resistivity (Griffiths and King, 1981).

The Vertical Electrical Sounding (VES) is one of the most important applications of the geoelectrical methods, which is principally used in areas where the geologic structure can be approximated by layers which are horizontal. The goal of (VES) is to determine from surface measurements at depths to the subsurface layers together with their electrical resistivities or conductivities (Orellana and Mooney, 1966).

The field estimations of hydraulic parameters of an aquifer are not always available; as a result, many investigation techniques were commonly employed to estimate the spatial distribution of its hydraulic parameters. The estimation of hydraulic conductivity (K) and Transmissivity (T_r) values from field pumping tests and down-hole well logging data, can however be very expensive and time consuming. In this context, surface geophysical (Resistivity Method) may provide rapid and effective techniques for groundwater exploration and aquifer evaluation (Batte et al., 2010).

The pumping tests that produce hydraulic conductivity results are often limited in number or, sometimes not well distributed over the whole study area. The obtaining of reliable values for the hydraulic conductivity of an aquifer is difficult due to lateral and vertical heterogeneities which are usually present in water-bearing geologic strata (El Idrysy and De Smedt, 2007). The complicated factors that effect on the resistivity values such as lithology and groundwater quality content cannot be differentiated by the geoelectric resistivity survey alone. Therefore, for an effective use of geoelectric resistivity data to the hydrogeological study, the correlation between real wells lithology data and the electrical field data is strongly recommended (George et al., 2011).

Bakkali and Amrani, 2008, used the different interpolation techniques on resistivity data to delineate subsurface phosphate aggregates referred by them as (phosphate disturbances) in Morocco. Anomalous zones of phosphate deposit "disturbances" correspond to resistivity anomalies. Much of the geophysical spatial analysis requires a continuous data set and their study is designed to create these surfaces. Such methods identified the best spatial interpolation for the creation of continuous resistivity data of phosphate disturbances zones. The effectiveness of this approach successfully reduced the noise which was accompanied by the analysis of stationary geophysical data as resistivity data (Bakkali and Amrani, 2008).

In the current geophysical study, six interpolation methods were exploited for hydrogeological aspects instead of phosphate aggregates, these methods are as follows: Kriging, Inverse distance to power, Natural neighbor, Minimum curvature, Triangulation interpolation with aspect ratio, and furthermore, polynomial regression calculated surface which was used to isolate residual resistivity from regional aquifer resistivity surface. The 1st directional derivative was used as a digital filter, which was applied on the residual resistivity field in order to delineate low resistivity and high hydraulic conductivity areas.

4. Material and method

After studying area geologically and topographically, a geophysical survey was designed to achieve 23 Schlumberger Vertical Electrical Sounding (VES) points distributed evenly across the study area. The Schlumberger sounding points were distributed with even spacing interval as much as possible about 1 km, Fig. 2, in order to form a good representative grid for the area. The applied Schlumberger array was oriented with the direction of (N45°W) and using the current electrodes spacing (AB), increased gradually from 80 to 1600 m, while potential electrodes (MN) increased gradually from 20 to 200 m far from the midpoint of each sounding point.

The Schlumberger array, (Fig. 3), was used by keeping the potential electrodes at a closer distance. The apparent resistivity (ρ_a) was determined using the following equation (Zohdy et al., 1990 in Batte et al., 2008):

$$\rho_a = \pi \left\{ \frac{\left(\frac{AB}{2}\right)^2 - \left(\frac{MN}{2}\right)^2}{MN} \right\} \Delta \frac{V}{I}$$

where AB = distance between the current electrodes in meters, MN = distance between potential electrodes in meters, ΔV = potential difference measured between the potential electrodes (volts), and I = the applied current strength.

The ABEM tetrameter LS Resistivity meter was used in the current survey.

After smoothing, resistivity curves were interpreted by attending the manual (Auxiliary Point Method) of partial matching using (Orellana and Mooney, 1966) two layers Schlumberger standard curves.

The sophisticated computer software for (VES) processing and interpretation (IPI2Win v.2.1) software was used to enhance the results through the reduction in the Root Mean Square (RMS%) between the calculated and the measured field curve as much as possible without affecting certain thickness layers, Fig. 4. The RMS% for the interpreted curves in this study was ranging between 2.4 and 5% according to the subsurface natural heterogeneity with best possible curve smoothing. The software uses the common forward and inversion technique should be carefully applied to give layers thickness as close as possible to the actual thickness values obtained from boreholes information.

The (VES) interpretation results represented the thickness (h) in meters and true resistivity (ρ) in (Ω m) for each geoelectrical layer of the (23) geoelectric columns located under the midpoints of each (VES) points in the study area.

The interpretation results presented as Geoelectrical sections along the profile (AA′) as shown in Fig. 5, extend from north to south, as shown in Fig. 2. The comparison between the boreholes lithology and sounding curves results made it possible to limit out the resistivity ranges and thickness variation for the lithological units in each profile. The existence of faulting and folding may highly affect the quality, distribution, flow directions, and amount of groundwater in the study area. This situation appears in the geoelectrical sections and isoresistivity maps of the region.

Heigold et al. (1979) constructed a relationship between hydraulic conductivity and aquifer resistivity by using the pumping test information of three wells for Niantic Illiopolis Aquifer, Fig. 6.

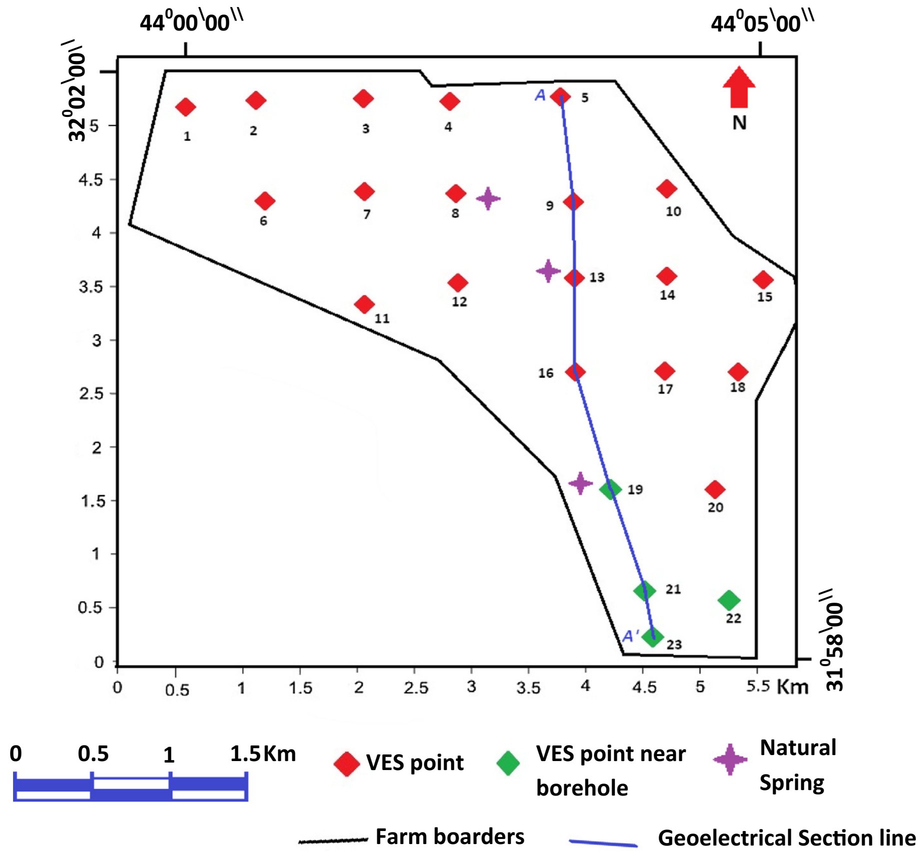

Figure 2 Geophysical survey design map.

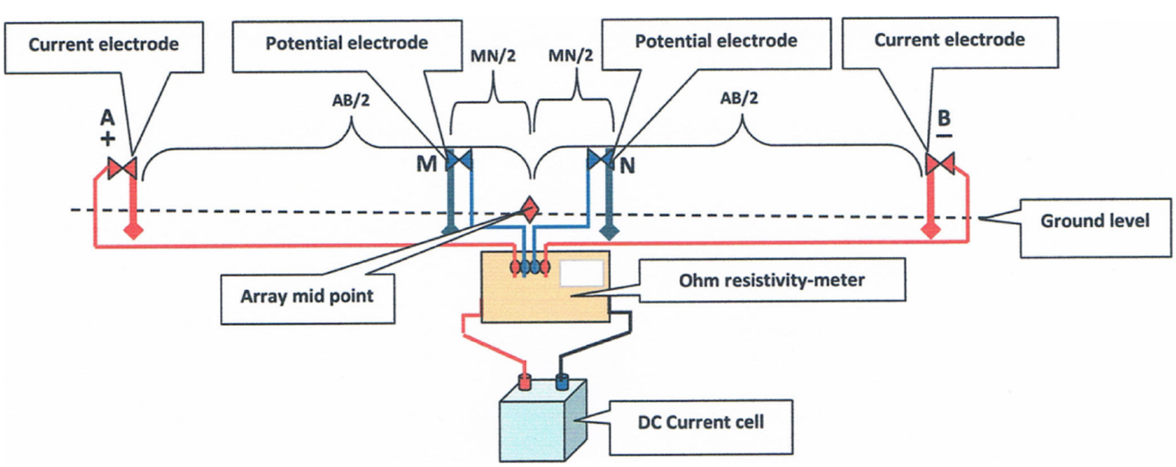

Figure 3 The electrode array for Schlumberger configuration at field resistivity survey (AlKhafaji, 2014).

An empirical statistical relation was conducted at the southern part of the study area. This part includes 8 VES points, four of them located near boreholes having results of pumping tests. Fig. 2 shows the location of these points. The relation was between the aquifer resistivity ($\rho_{Aq.}$) and hydraulic conductivity is shown in Fig. 7.

Both linear and polynomial trends applied to present the function between the two parameters and to conduct the equation which was used later to predict (K) values for other sounding points in the area where no pumping test was achieved. The second relation was proposed between ($\rho_{Aq.}$) and (T_r) Fig. 8.

Equations were conducted either and used later to predict (T_r) values at locations of other VES points where no pumping test was achieved.

Both empirical relations ($\rho_{Aq.}$ vs. K) and ($\rho_{Aq.}$ vs. T_r), showed relatively a high correlation coefficients (R) values, which are 0.92 and 0.83 consequently. Therefore, equations

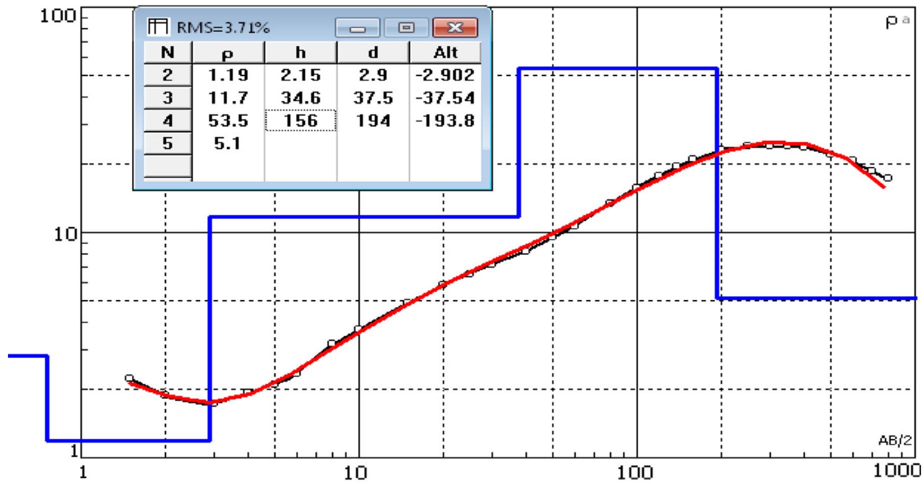

Figure 4 The enhanced interpretation for one of the VES points.

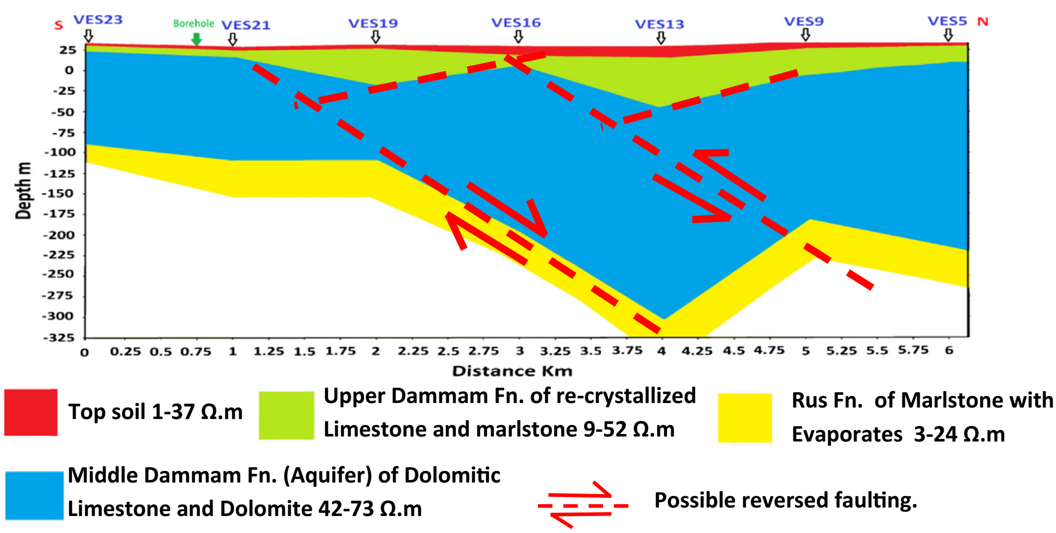

Figure 5 Geoelectrical section A-A′ across the study area showing possible reversed faulting.

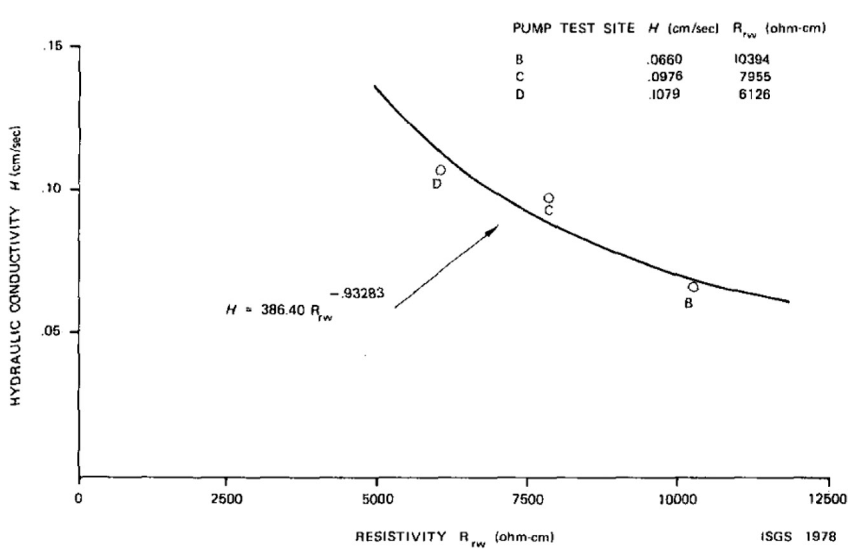

Figure 6 Hydraulic conductivity and aquifer resistivity relationship along the axis of Niantic Illiopolis Aquifer (Heigold et al., 1979).

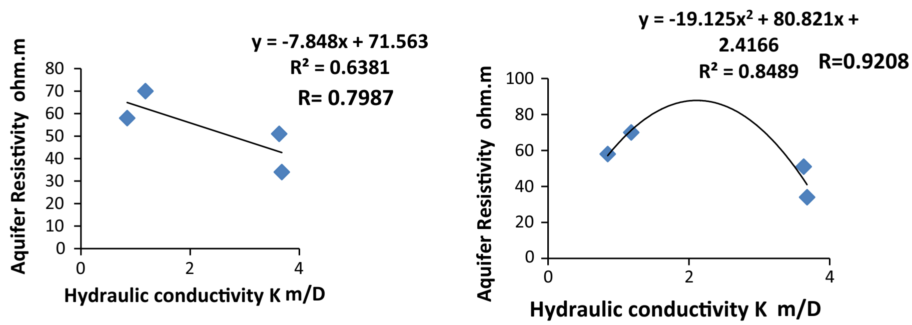

Figure 7 Statistical empirical relations between Aquifer resistivity ($\rho_{Aq.}$) and hydraulic conductivity (K) for four locations at the southern part of the study area.

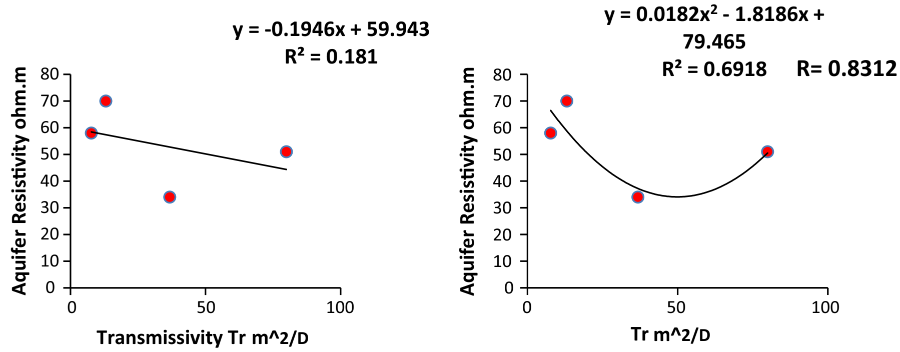

Figure 8 Statistical empirical relations between Transmissivity (T_r) and Aquifer resistivity ($\rho_{Aq.}$) for four locations at the southern part of the study area.

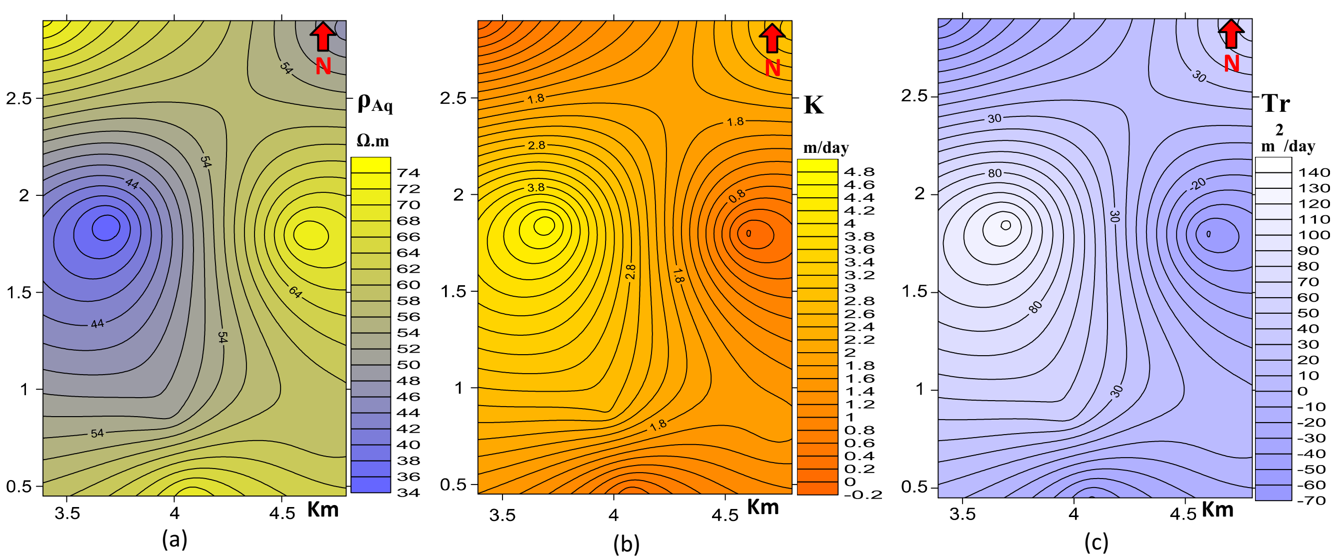

Figure 9 Comparison among the following: (a) Aquifer resistivity ($\rho_{Aq.}$), (b) hydraulic conductivity (K), and (c) Transmissivity (T_r) at the southern part of the study area.

conducted by those two relations have been used to integrate K and T_r values for the other sounding point locations in the study area.

Contour map of ($\rho_{Aq.}$), for the southern part drew and was compared with predicted K and T_r, to show high similarity in anomalies locations among the three maps, Fig. 9.

Aquifer related contour and colored 2d surfaces were drawn by using the Surfer software which was produced by Golden Software Company by applying Kriging method, Fig. 10.

It was found that there is a retrograde inverse empirical relation between ($\rho_{Aq.}$) and (K), at the study area, Fig. 7.

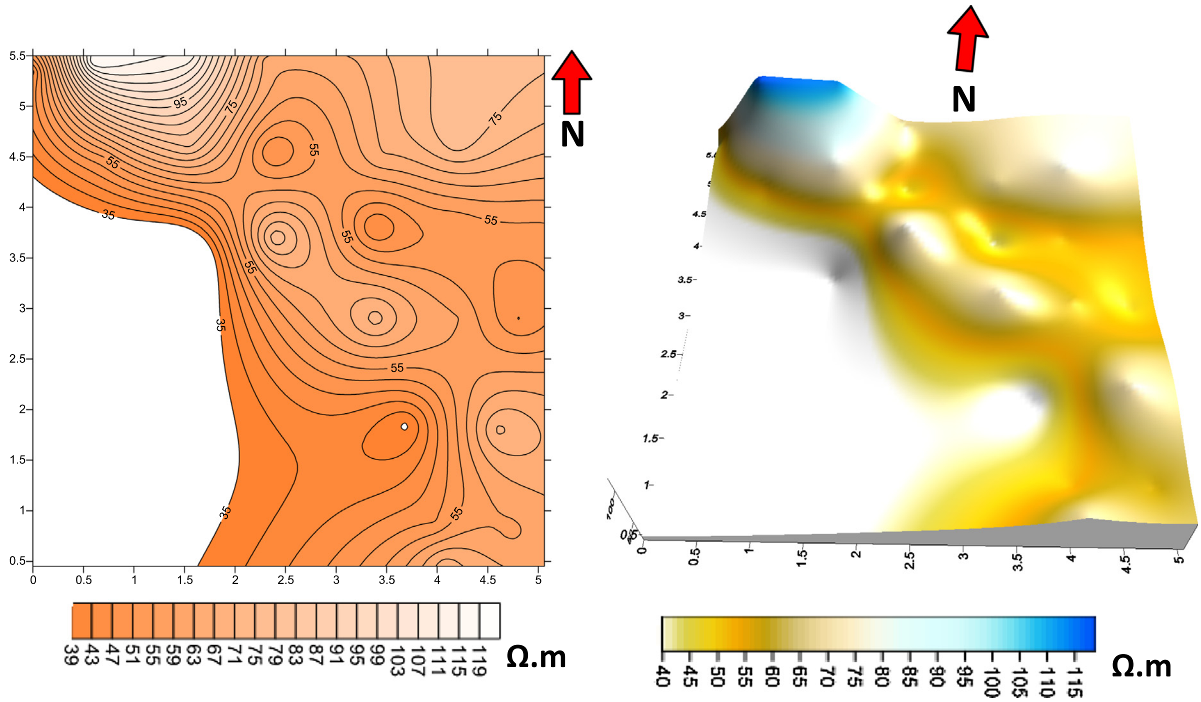

Figure 10 Aquifer resistivity ($\rho_{Aq.}$) map and 2D surface for the study area.

Therefore, zones of low ($\rho_{Aq.}$) in Fig. 10, appear as ridges in the predicted (K) surface of Fig. 11, which drew also by using the ordinary Kriging method.

The zones of high (K) in map of Fig. 11, could be used to predict the groundwater flowing directions which appear as red arrows in the surface of Fig. 11.

Six spatial interpolation methods are applied on the same ($\rho_{Aq.}$) data in order to find the best surface visualization and least noise to clarify zones of high (K) and (T_r) at the study area, Fig. 12.

Each method visualized data in a different manner from the other in a way, and the aim was to clarify some aquifer properties graphically by reducing noise and ambiguity related to lithology heterogeneities as much as possible.

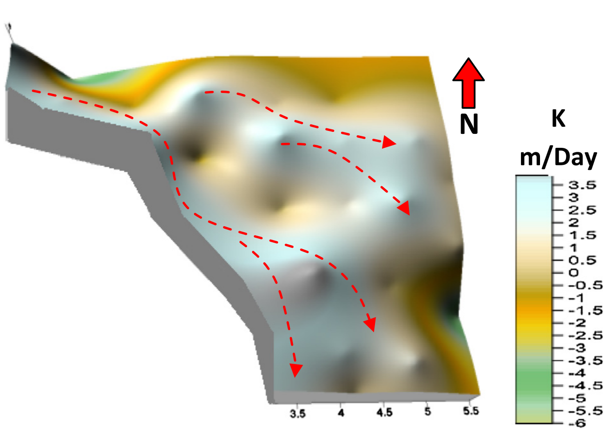

Figure 11 The predicted Hydraulic conductivity (K) 2D surface for the study area .

It was proposed to process the aquifer resistivity map which represents the electrical zone related to the groundwater aquifer specifically. By try and error 1st, 2nd and 3rd polynomial orders were applied, but the best results were given when the 2nd order polynomial regression was applied. By applying the 2nd order polynomial regression on the aquifer resistivity contour map, Fig. 13a, it was possible to obtain the regional map of aquifers resistivity, Fig. 13b.

By subtracting data point values of map in Fig. 13a from those which belong to the map of Fig. 13b, the result would be a new surface, Fig. 13c and d, and this new surface represents the residual aquifer resistivity map. The residual aquifer resistivity surface has a negative and positive resistivity values around the regional surface where points have the resistivity value of (0 Ω m).

The negative residual resistivity regions refer to high (K) values, as ($\rho_{Aq.}$) and (K) are in an inversely proportional relation. This was helpful in zoning areas of high (K) values, and such zones are important in locating drilling positions of any future groundwater investment wells. Satisfactory regions appear as a green zone with a residual resistivity ranging between 0 and 20 Ω m in the map of Fig. 13c.

As the 0 value contour line in Fig. 13c represents the regional resistivity level, then it might be considered as a limit that separate positive and negative residual ($\rho_{Aq.}$) zones. In other words this boarder line delineates locations of sudden ($\rho_{Aq.}$) variations within the aquifer. Such sudden variations may reflect the locations of faulting within the carbonate rocks of the aquifer, where ($\rho_{Aq.}$) and (K) values alter on both sides of these faults. The faulting actions are confirmed by previous studies especially for those with the directions NW-SE and N–S, and that is what sensed when observing the residual ($\rho_{Aq.}$) surface, Fig. 14.

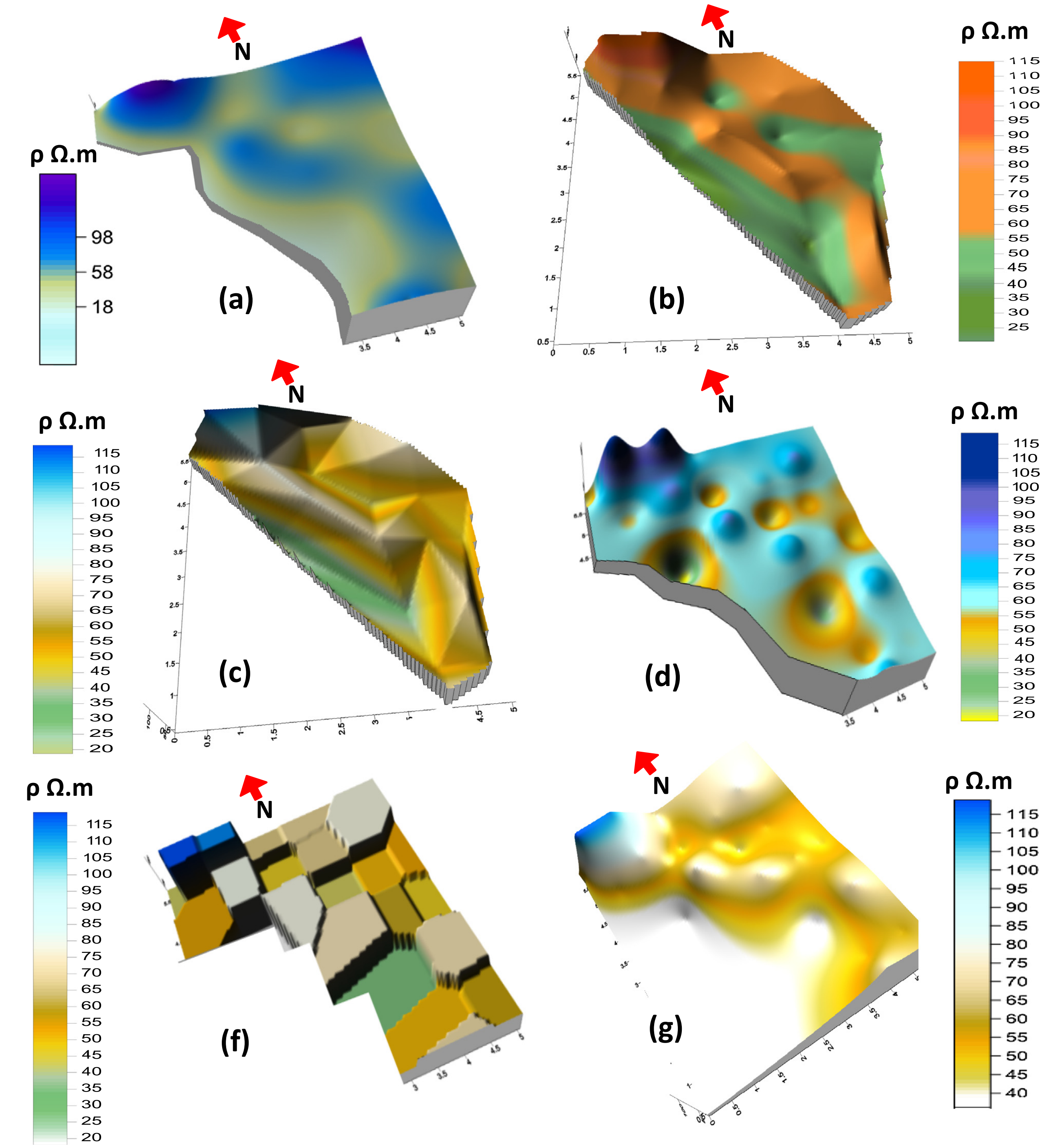

Figure 12 Six different interpolation methods used to visualize ($\rho_{Aq.}$) for the study area, (a) minimum curvature, (b)natural neighbor, (c) Triangulation with aspect ratio 3, (d) inverse distance to power 2, (f) nearest neighbor with research ellipse 7.15, and (g) Kriging method.

Another try made to reduce the data related noise was proposed by applying the 1st derivative filter on the residual ($\rho_{Aq.}$) surface with the direction of 45° NE-SW, and this direction was perpendicular on the prevalent NW-SE faulting direction in the study area. The result was presented as a surface as it is shown in Fig. 15.

The 1st directional derivative filtered surface delineated the zones of low resistivity or high hydraulic conductivity which appears in green inside Fig. 15. The intersection of faults may cause the final shape of this low resistivity zone, and this green pinch may represent a graben fault within the carbonate rocks of the aquifer.

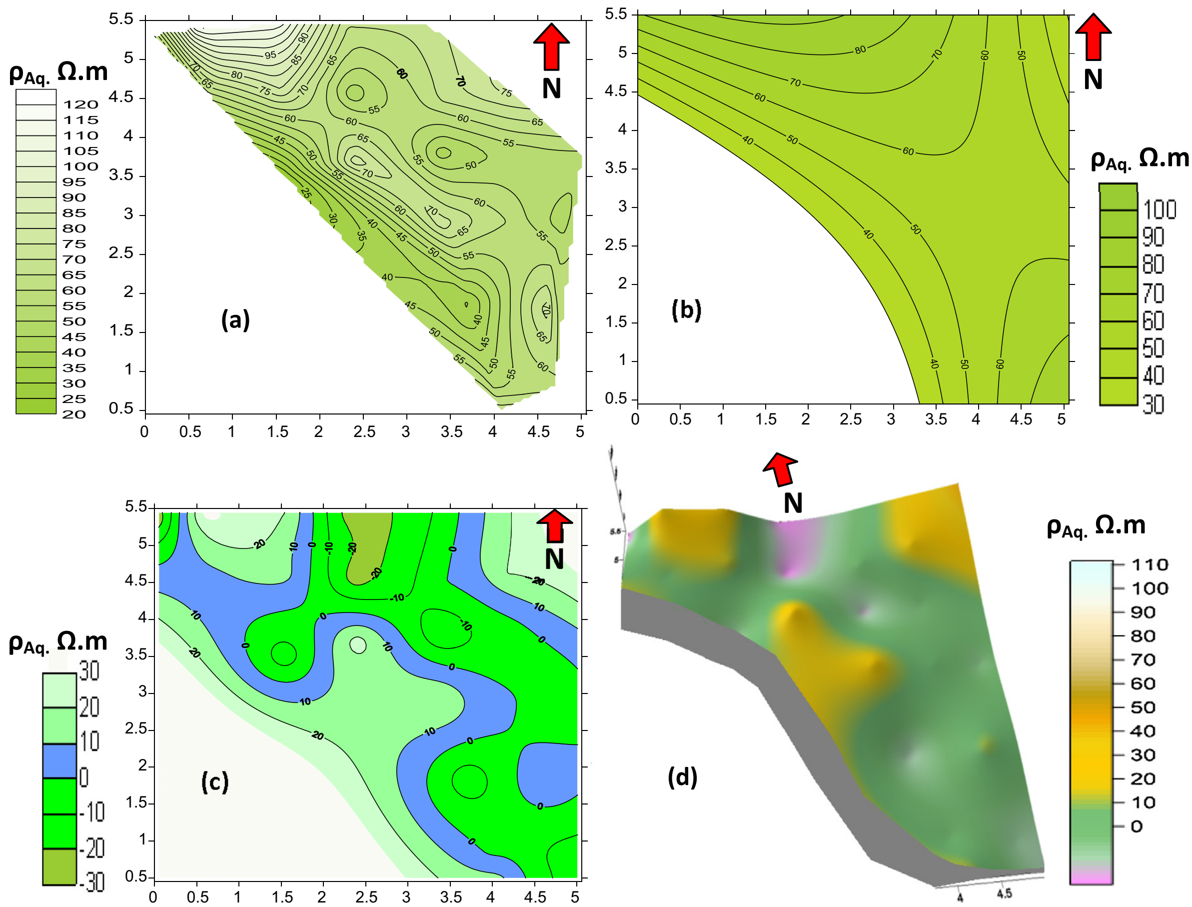

Figure 13 The application of polynomial regression on ($\rho_{Aq.}$) for the study area: (a) ($\rho_{Aq.}$) map; (b) regional ($\rho_{Aq.}$) by applying 2nd order polynomial regression; (c) residual ($\rho_{Aq.}$) contour map; (d) residual ($\rho_{Aq.}$) surface.

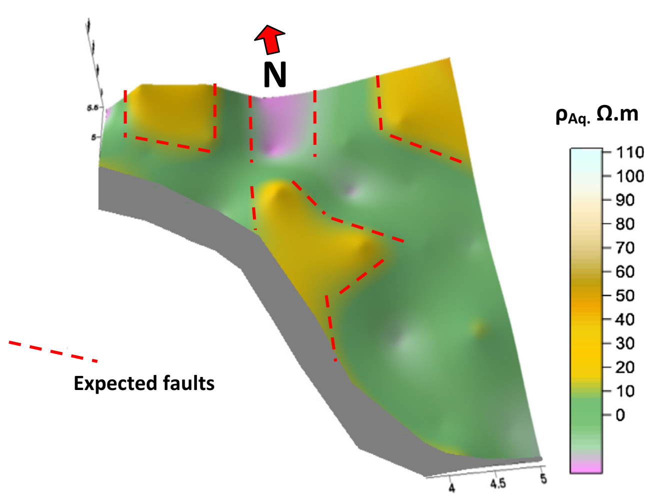

Figure 14 Expected faults observed on the residual ($\rho_{Aq.}$) surface.

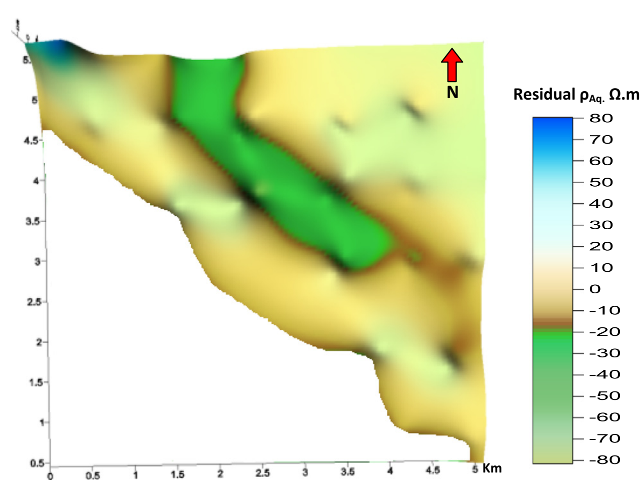

Figure 15 The application of 1st directional derivative filter on the residual ($\rho_{Aq.}$) surface.

5. Conclusions

The empirical statistical relation between ($\rho_{Aq.}$) and (K) is inversely proportional for the studied aquifer, so that positive ($\rho_{Aq.}$) anomalies become negative (K) anomalies when transformed to a predicted K surface. The predicted (K) surface drew by using the ordinary Kriging interpolation method and provided a better vision about the expected flowing directions of groundwater. Among the six applied interpolation methods, minimum curvature and natural neighbor were the most helpful in zoning high and low ($\rho_{Aq.}$) extensions within the study area. The 2nd order polynomial regression was helpful in calculating the residual ($\rho_{Aq.}$) graphical surface. This surface zoned the area more precisely into a positive and negative ($\rho_{Aq.}$) anomalies around the regional surface. Furthermore, the residual ($\rho_{Aq.}$) surface was very helpful in assigning sudden linear variations, which was proposed as faulting lines. The 1st directional derivative filter was applied on the residual ($\rho_{Aq.}$) surface to produce an enhanced surface to assign limits of low resistivity or high hydraulic conductivity zones.

References

Al-Khafaji, W.M.S., 2014. A geophysical study to evaluate the groundwater reserve and structural situation os south Sinjar anticline region – NW Iraq Ph.D. dissertation. University of Baghdad – College of Science – Department of Geology, 171 pages.

Bakkali, S., Amrani, M., 2008. About the use of spatial interpolation methods to denoising Moroccan resistivity data phosphate "Disturbances" map. Acta Montanistica Slovaca Ročník 2 (13), 216–222.

Barawary, A.M., Slewa, N.A., 1994. The geology of Al-Najaf quadrangle sheet NH-38-2. The State Establishment of Geological Survey and Mining. Iraq. 20 pages (unpublished report).

Batayneh, A.T., 2009. A hydrogeophysical model of the relationship between geoelectric and hydraulic parameters, Central Jordan. J. Water Resour. Protect. 1, 400–407.

Batte, A.G., Barifaijo, E., Kiberu, J.M., Kawule, W., Muwanga, A., Owor, M., 2010. Correlation of geoelectric data with aquifer parameters to delineate the groundwater potential of hard rock Terrain in Central Uganda. Pure Appl. Geophys. 167, 1549–1559. http://dx.doi.org/10.1007/s00024-010-0109-x, Springer Basel AG.

Batte, A.G., Muwanga, A., Sigrist, W.P., 2008. Evaluating the use of vertical electrical sounding as a groundwater exploration technique to improve on the certainty of borehole yield in Kamuli District (Eastern Uganda). Afr. J. Sci. Technol. (AJST) Sci. Eng. Ser. 9 (1), 72–85.

Buday, T., Jassim, S.Z., 1987. The Regional Geology of Iraq. In: Tectonism, Magmatism and Metamorphism, vol.2. Publication of GEOSURV, Baghdad, p. 352.

El Idrysy, H., De Smedt, F., 2007. A comparative study of hydraulic conductivity estimations using geostatistics. Hydrogeol. J. (15), 459–470

George, N.J., Obianwu, V.I., Obot, I.B., 2011. Estimation of groundwater reserve in unconfined frequently exploited depth of aquifer using a combined surficial geophysical and laboratory techniques in The Niger Delta, South – South, Nigeria. Pelagia Research Library (USA) AASRFC. Adv. Appl. Sci. Res. 2 (1), 163–177.

Griffiths, D.H., King, R.F., 1981. "Applied Geophysics for Geologists and Engineers" the Elements of Geophysical Prospecting, second ed. Pergamon Press, 201 pages.

IpI2Win v. 2.1 Users Guide, 2001. A computer software user guide catalog presented by Moscow State University, Geological Faculty, Department of Geophysics and Geoscan-m Ltd., P.25.

Heigold, P.C., Gilkeson, R.H., Cartwright, K., Reed, P.C., 1979. Aquifer transmissivity from surficial electrical methods. Ground Water 17 (4), 338–345.

Jassim, S.Z., Goff, J.C., 2006, Geology of Iraq. In: Dolin, Hlavni 2732, Prague and Moravian Museum, Zelny trh 6, Brno, Czech Republic, first ed. 341 pages.

Keller, G., Frischknecht, F., 1966. Electrical Methods in Geophysical Prospecting. Pergamon, NY.

Orellana, E., Mooney, H.M., 1966, Master Curves for Schlumberger Arrangement, Madrid, p. 34.

Sharma, P.V., 1986. Geophysical Methods in Geology. Elsevier Science Publishing Co., Inc., Amsterdam, The Netherlands, 442 pages.

Zohdy, A.A.R., Eaton, G.P., Mabey, D.R., 1990. Application of surface geophysics to ground-water investigations. Techniques of Water-Resources Investigations of the United States Geological Survey, fourth ed., U.S.G.S., p. 123.